



Original Article

Effects of urea, metal ions and surfactants on the binding of baicalein with bovine serum albumin[☆]Atanu Singha Roy^{*}, Amit Kumar Dinda, Nitin Kumar Pandey, Swagata Dasgupta

Department of Chemistry, Indian Institute of Technology, Kharagpur 721302, India

ARTICLE INFO

Article history:

Received 5 August 2015

Received in revised form

1 April 2016

Accepted 5 April 2016

Available online 20 April 2016

Keywords:

Bovine serum albumin (BSA)

Baicalein

Binding constant

Fluorescence spectroscopy

Molecular docking

ABSTRACT

The interaction of baicalein with bovine serum albumin (BSA) was investigated with the help of spectroscopic and molecular docking studies. The binding affinity of baicalein towards BSA was estimated to be in order of 10^5 M^{-1} from fluorescence quenching studies. Negative ΔH° ($-5.66 \pm 0.14 \text{ kJ/mol}$) and positive (ΔS°) ($+79.96 \pm 0.65 \text{ J/mol K}$) indicate the presence of electrostatic interactions along with the hydrophobic forces that result in a positive ΔS° . The hydrophobic association of baicalein with BSA diminishes in the presence of sodium dodecyl sulfate (SDS) due to probable hydrophobic association of baicalein with SDS, resulting in a negative ΔS° ($-40.65 \pm 0.87 \text{ J/mol K}$). Matrix-assisted laser desorption ionization/time of flight (MALDI-TOF) experiments indicate a 1:1 complexation between baicalein and BSA. The unfolding and refolding phenomena of BSA were investigated in the absence and presence of baicalein using steady-state and fluorescence lifetime measurements. It was observed that the presence of urea ruptured the non-covalent interaction between baicalein and BSA. The presence of metal ions (Ag^+ , Mg^{2+} , Ni^{2+} , Mn^{2+} , Co^{2+} and Zn^{2+}) increased the binding affinity of ligand towards BSA. The changes in conformational aspects of BSA after ligand binding were also investigated using circular dichroism (CD) and Fourier transform infrared (FT-IR) spectroscopic techniques. Site selectivity studies following molecular docking analyses indicated the binding of baicalein to site 1 (subdomain IIA) of BSA.

© 2016 Xi'an Jiaotong University. Production and hosting by Elsevier B.V. This is an open access article under the CC BY-NC-ND license (<http://creativecommons.org/licenses/by-nc-nd/4.0/>).

1. Introduction

The highly abundant carrier proteins of blood plasma are serum albumins. They are responsible for the transportation and distribution of various exogenous and endogenous substances in blood. They possess an ability to complex with different biologically active compounds such as drug molecules, fatty acids, hormones, and dyes in the body [1,2]. Bovine serum albumin (BSA) is a globular protein like human serum albumin and has about 76% structural homogeneity to human serum albumin [3]. It comprises three structurally homologous domains (I, II, III), each of which is further divided into subdomains A and B. Each of the domains is separated into nine loops (L1-L9) with the help of 17 disulfide bonds. [3–5]. Site 1 and site 2 are situated in subdomain IIA and IIIA, respectively [3,6]. They are generally called the warfarin and ibuprofen binding sites, respectively [3,6]. Site 1 has an inclination for bulkier heterocyclic polar substances, while site 2 generally favors small aromatic carboxylic acids [7]. BSA has two tryptophan

residues (Trp 134 and Trp 213), among which Trp 213 is situated in a hydrophobic pocket (site 1, subdomain IIA) and Trp 134 is placed on the surface region of BSA [3,4,8].

Depending on the potent anti-oxidant, anti-tumor, anti-inflammatory and anti-cancer activities of several naturally occurring compounds belonging to the flavonoid family, a large number of publications have been reported recently by various research groups [9–12]. The flavone baicalein (5,6,7-trihydroxyflavone, Fig. 1), isolated from *Scutellaria baicalensis* Georgi, is capable of reducing the growth of human cancer cells [12]. Baicalein is found to inhibit the lipoxygenases and reduce cell damage by reactive oxygen species [13]. Baicalein can protect mice from metabolic syndrome (persuaded by an elevated fat diet in mice) through an AMPK α (2)-mediated pathway that involved different intracellular signaling paths [14]. It is found to prevent the growth of hepatocellular carcinoma cell via inhibiting MEK-ERK signaling pathway [15]. Baicalein is also reported to act as a neuroprotective and anti-fibrotic agent in the field of pharmacology [16,17]. Serum albumins have the abilities to bind a wide range of small drugs to facilitate the procedures of drug disposition, transportation and metabolism. The reversible nature of interaction has a direct consequence in the delivery of these compounds and their metabolites to cells and tissues [18]. Hence, the binding of baicalein with BSA has

[☆]Peer review under responsibility of Xi'an Jiaotong University.

^{*} Correspondence to: Department of Chemistry, National Institute of Technology Meghalaya, Shillong 793003, India.

E-mail addresses: singharoyatanu@gmail.com, asroy86@nitm.ac.in (A.S. Roy).

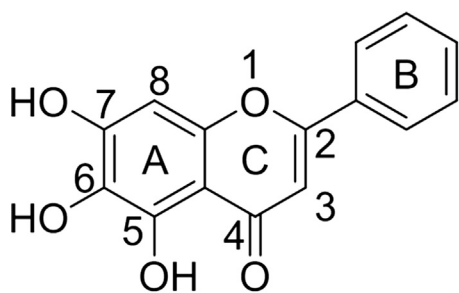


Fig. 1. Structure of baicalein.

significant effect on the understanding of binding affinity, mode of binding and its relative bioavailability [19].

The interaction of baicalein with BSA in 20 mM Tris–HCl buffer of pH 7.4 was reported using fluorescence spectroscopy by Li et al. [20]. However, the effect of surfactants on the binding of baicalein with BSA has not been previously looked into. To further probe the specific forces of interaction involved in the process, the interaction studies were also performed with varying ionic strength. In this study we probed the interactions of baicalein with BSA using the following techniques: UV–vis, steady-state fluorescence, circular dichroism (CD), Fourier transform infrared spectroscopy (FT-IR) and matrix-assisted laser desorption/ionization/time of flight (MALDI–TOF) analyses. Thermodynamic parameters (ΔH° , ΔS° and ΔG°) were estimated from the binding constant values at four different temperatures. The unfolding and refolding of BSA were carried out using the chemical denaturant urea in the absence and presence of baicalein. Finally, molecular docking studies were conducted to get an idea about the residues involved in the binding.

2. Materials and methods

2.1. Materials

BSA (fraction V), baicalein, TX-100, warfarin and ibuprofen were purchased from Sigma Co. (St. Louis, MO, USA). SDS, cetyltrimethylammonium bromide (CTAB) and other analytical grade reagents were acquired from Sisco Research Laboratory, India. The concentration of BSA was measured spectrophotometrically (Shimadzu UVPC 2450) by dissolving it in 20 mM phosphate buffer of pH 7.0 using a molar extinction coefficient of $43800 \text{ M}^{-1} \text{ cm}^{-1}$ at 280 nm [21]. The concentrations of baicalein, warfarin and ibuprofen were determined on a Shimadzu UVPC 2450 using their respective molar extinction coefficients: ϵ_{323} (baicalein) in ethanol = $15700 \text{ M}^{-1} \text{ cm}^{-1}$, ϵ_{308} (warfarin) = $12500 \text{ M}^{-1} \text{ cm}^{-1}$ [22], and ϵ_{222} (ibuprofen) = $12700 \text{ M}^{-1} \text{ cm}^{-1}$ [23]. All the experiments were performed in phosphate buffer containing less than 5% alcohol.

2.2. UV–vis study

UV–vis studies for the interaction of baicalein with BSA were carried out on the Shimadzu UVPC 2450 spectrophotometer (Shimadzu Corporation, Tokyo, Japan) at 25 °C in the range of 200–500 nm using a 1 cm quartz cuvette in 20 mM phosphate buffer of pH 7.0. A 1 mL aliquot of 20 μM baicalein in phosphate buffer was titrated with consecutive addition of BSA (0, 2.5, 5.0, 7.5, 10, 12.5, 15, 17.5 and 20 μM). Titrations were performed manually with the help of micro-pipette.

2.3. Fluorescence spectroscopy

The fluorimetric measurements were performed on a Horiba

Jobin Yvon spectrofluorimeter (Fluoromax 4 from Horiba Kyoto, Japan) with a 1 cm quartz cell. Aliquots of 3 mL of 2 μM BSA were titrated with the addition of baicalein (0, 1.2, 2.4, 3.6, 4.8, 6.0, 7.2, 8.4, 9.6, 10.8 and 12 μM) at four temperatures (20, 26, 32 and 39 °C) in 20 mM phosphate buffer of pH 7.0. Similar experimental techniques were reported by Li et al. [20]. The fluorescence spectra were collected using an excitation wavelength of 295 nm and emission wavelength in the range of 305–500 nm. The blank spectra were recorded and subtracted from each BSA–baicalein complex spectrum. The binding of baicalein with BSA was also checked in the presence of different potassium chloride (KCl) concentrations. To see the effect of surfactants on the binding of baicalein with BSA, the same experiments were performed in the presence of SDS, CTAB and TX-100. The concentrations of the surfactants ([SDS]=8.5 mM, [CTAB]=1.1 mM and [TX-100]=0.035 mM) were taken above their critical micelle concentration (CMC) in water ([CMC_{SDS}]=8.2 mM, [CMC_{CTAB}]=0.92–1.0 mM and [CMC_{TX-100}]=0.22–0.24 mM).

The binding constants were also analyzed in the presence of some common metal ions (Ag^+ , Ca^{2+} , Mg^{2+} , Ni^{2+} , Mn^{2+} , Co^{2+} , Zn^{2+} and Cu^{2+}). The solutions containing the protein (2 μM) and the metal ions (100 μM) were incubated for 1 h, and titrated with successive addition of baicalein (0–12 μM) at 26 °C in 20 mM phosphate buffer of pH 7.0.

The three-dimensional (3D) spectroscopic experiments were performed on a Hitachi F-7000 spectrofluorometer. The fluorescence spectra of BSA (5 μM) in the absence and presence of baicalein (25 μM) were obtained using excitation and emission collected in the range of 200–380 nm and 250–500 nm respectively with a 10 nm increment using excitation and emission slit widths fixed at 5 nm.

2.4. Site-selectivity study

Warfarin (2 μM) and ibuprofen (2 μM) were incubated with BSA for 1 h in phosphate buffer of pH 7.0. The samples were excited at 295 nm (Both excitation and emission slit widths were fixed at 2 nm) and titrated with the consecutive addition of baicalein (0–12 μM). The binding constant values of baicalein with BSA in the presence of these warfarin and ibuprofen were calculated using the Eq. (3) as described later.

2.5. Fluorescence resonance energy transfer

The fluorescence quenching spectrum of a 1:1 baicalein–BSA complex was collected using $\lambda_{\text{ex}}=295 \text{ nm}$ in the range of 305–500 nm under similar experimental conditions. The UV–vis spectrum of 2 μM baicalein at pH 7.0 was recorded on the same spectrophotometer at 25 °C in the range of 200–500 nm using a 1 cm quartz cuvette.

2.6. MALDI–TOF measurements

The mass spectra were collected on a MALDI–TOF instrument (Voyager–De Pro from Applied Biosystems, USA) in positive ion mode. Free BSA (20 μM) and BSA–baicalein complex (20 μM :120 μM) samples were prepared in experimental buffer and incubated for 12 h. The samples were mixed with the matrix solution (20 mg/mL sinapinic acid was dissolved in mixture of water and HPLC grade acetonitrile containing 0.1% trifluoroacetic acid) in the ratio of 50:50 (v/v). The sample solutions were then spotted on the steel plate and left for 6 h. MALDI–TOF scanning was executed keeping the accelerating voltage at 25 kV and mass range over an m/z from 20 to 120 kD.

2.7. CD measurements

Far-UV CD experiments were carried out on a Jasco-810 automatic spectrophotometer (Japan Spectroscopic Society, Japan) using a 0.1 cm cell path length at room temperature. The spectra were scanned in the region of 190–240 nm with a speed of 50 nm/min and a response time of 4 s. Three different sets of protein sample (BSA to baicalein molar ratio: 1:0, 1:1 and 1:2) were prepared in buffer. All the CD spectra were corrected with respect to the blank samples. Secondary structural components of protein were calculated with the help of DICHROWEB [24].

2.8. Fourier transform infrared spectroscopy

FT-IR experiments were executed on a Nexus 870 FT-IR spectrometer (Thermo Nicolet Corporation, Berkeley, USA) equipped with a zinc selenide (ZnSe) attenuated total reflectance (ATR) accessory, a deuterated triglycine sulfate (DTGS) detector and a KBr beam splitter at room temperature. 15 mg/mL BSA was dissolved in 20 mM phosphate buffer and three sets of solutions containing the BSA:baicalein in different molar ratios (1:0, 1:1 and 1:2) were prepared. A 256-scan interferogram with 4 cm^{-1} resolution was used to obtain the spectra after 2 h sample incubation. Blank spectra were acquired similarly and subtracted from each to get the different spectra.

Using the method reported by Byler and Susi [25], the secondary structures of BSA and BSA-baicalein complexes were estimated from FT-IR data using the position of amide I band ($1700\text{--}1600\text{ cm}^{-1}$). To reduce the noise the corrected spectra were smoothed by a 15-point Savitsky-Golay smooth function [25]. Fourier self deconvolution and second derivative calculation of the smoothed spectra were used to resolve the major peaks. The Gaussian curve fitting method was implemented in the region of $1700\text{--}1600\text{ cm}^{-1}$ to estimate the total area and area corresponding to each component of secondary structure.

2.9. Unfolding and refolding phenomena of BSA

Studies on urea (0–7 M) induced chemical denaturation of BSA in the absence and presence of baicalein were performed with the help of steady-state fluorescence spectroscopy and lifetime measurements. The BSA (15 μM) and baicalein-BSA (15 μM :15 μM) systems were excited at 295 nm and the emission was collected in the range of 300–500 nm. The fluorescence lifetime measurements were carried out on an EasyLife™ V instrument obtained from Optical Building Blocks Corporation. The instrument is equipped with a pulsed width of 1.5 ns and the decay data of the samples were analyzed using the same software of the instrument. The fluorescence decays of the samples were recorded in the region of 60–120 ns with an average of 20 using 200 channels. The excitation wavelength was 295 nm to excite specifically tryptophan residues of the protein. The average life-time (τ) can be expressed according to the following Eq. (1).

$$\langle \tau \rangle = a_1\tau_1 + a_2\tau_2 \quad (1)$$

2.10. Molecular docking

The 3D crystal structure of BSA (PDB ID: 4F5S) [26] was obtained from the Protein Data Bank [27]. The energy minimized structures of baicalein and its anion were developed in Sybyl 6.92 (Tripos Inc., St. Louis, USA) using MMFF94 force field and MMFF94 charges. The docking of baicalein and its anion with BSA was performed using FlexX, available in the Sybyl suite and the docked pose was visualized using PyMol [28].

NACCESS was used to calculate the accessible surface area (ASA) of free and complexed BSA [29]. The change in ASA for the *j*th residue was calculated using $\Delta ASA^j = ASA^j(\text{free BSA}) - ASA^j(\text{baicalein-BSA})$. If the loss in ASA of a residue is greater than 10 \AA^2 , it indicates involvement of that residue in the binding [30].

3. Results and discussion

3.1. UV-vis spectral studies

Flavonoids demonstrate two bands, band II (240–280 nm) and band I (300–400 nm) due to benzoyl (A+C) and cinnamoyl (B+C) moieties, respectively [31]. The UV-vis spectrum of baicalein shows two distinct bands at 275 and 338 nm at pH 7.0. Band I is red shifted (25 nm) in the presence of BSA (Fig. 2A), suggesting the presence of a specific interaction between BSA and baicalein. The spectral broadening of baicalein in the presence of BSA may be due to the presence of specific, non-covalent interaction with the amino acid residues [32]. The ground state equilibrium constant (K_a) for 1:1 complexation between baicalein and BSA at 25 °C was estimated according to the Benesi-Hildebrand equation [33].

$$\frac{1}{\Delta A} = \frac{1}{(\epsilon_b - \epsilon_f)L_T} + \frac{1}{(\epsilon_b - \epsilon_f)L_T K_a [BSA]} \quad (2)$$

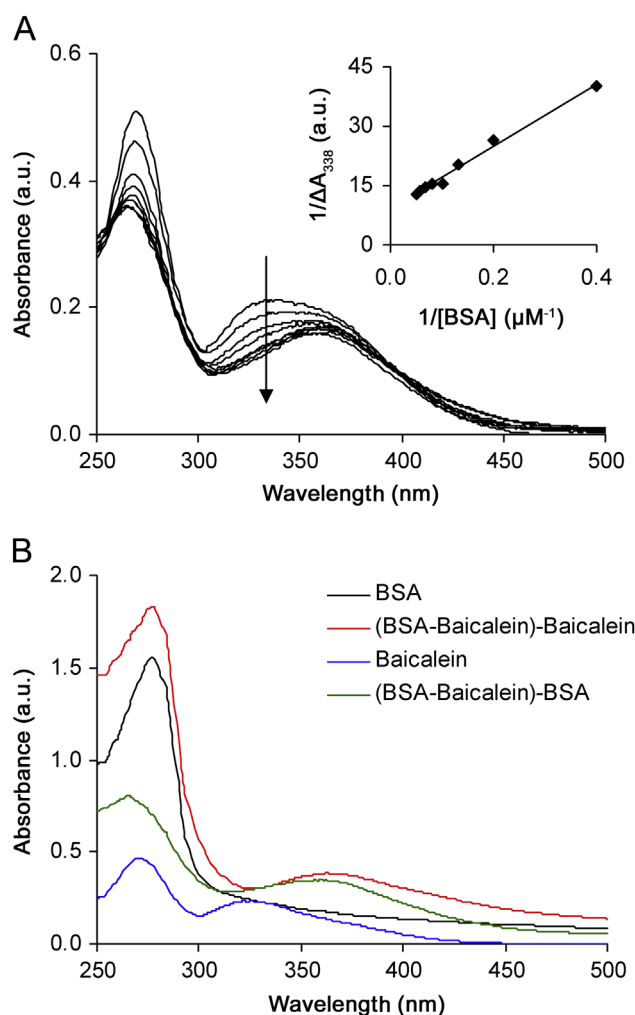


Fig. 2. (A) UV-vis spectra of baicalein (20 μM) in the absence and presence of BSA 0–20 μM) in 20 mM phosphate buffer of pH 7.0 (Inset: corresponding Benesi-Hildebrand plot) and (B) UV-vis spectra of baicalein, BSA and BSA-baicalein complexes under the same experimental condition. $[BSA] = [Baicalein] = 25\text{ }\mu\text{M}$.

where the subscripts T , b and f refer to total, bound and free ligand. $[BSA]$ is the concentration of BSA and L_T represents the total ligand concentration. The ΔA is the change in the absorbance at a particular wavelength. From the plot of $1/\Delta A$ versus $1/[BSA]$, it is possible to determine the association constants (K_a) for the binding, estimated from the ratio of the intercept and the slope (inset of Fig. 2A). The ground state equilibrium constant (K_a) was found to be $(1.17 \pm 0.91) \times 10^5 \text{ M}^{-1}$ ($R^2=0.99$) using the ΔA at 338 nm.

3.2. Fluorescence quenching mechanism

Fluorescence emission spectra of the protein in the absence and presence of increasing baicalein concentration are given in Fig. 3A. Baicalein did not exhibit any fluorescence property under the experimental conditions. The inherent fluorescence of BSA quenched considerably in the presence of baicalein. The blue shift (6 nm) in emission spectra after addition of baicalein is an indication of the presence of hydrophobic interaction between baicalein and BSA. The quenching mechanism involved here was discussed with the help of the Stern-Volmer Eq. (3) [34].

$$\frac{F_0}{F} = 1 + K_q \tau_0 [Q] = 1 + K_{SV} [Q] \quad (3)$$

where F_0 and F are the fluorescence emission intensities of BSA in the absence and presence of baicalein, K_q represents the bimolecular quenching constant and τ_0 (5 ns [10]) is the lifetime of the fluorescence in the absence of quencher. K_{SV} and $[Q]$ are the Stern-Volmer quenching constant and the quencher concentration. The K_{SV} values were obtained by plotting F_0/F versus $[Q]$ at four temperatures (Fig. 3B). The Stern-Volmer quenching constants (K_{SV}) at different temperatures were obtained from the slope of the Stern-Volmer curve (Fig. 3B) and K_q was calculated by using the following expression $K_{SV} = K_q \tau_0$. The quenching parameters at four different temperatures are summarized in Table 1. It was observed that an increase in temperature causes a decrease in K_{SV} values. K_{SV} and K_q were found in the order of 10^5 M^{-1} and $10^{13} \text{ M}^{-1} \text{ s}^{-1}$, respectively, which matched well with the reported values [20]. This is an indication of the presence of a static quenching mechanism. The values of K_q are greater than the limiting value of $2 \times 10^{10} \text{ M}^{-1} \text{ s}^{-1}$ [34], which is the maximum possible value of dynamical quenching constant in aqueous medium.

In addition, the UV-vis data show that the absorption spectrum of BSA does not overlap with the BSA-baicalein complex spectrum

Table 1

The quenching and binding parameters for the interaction of baicalein with BSA at different temperatures.

Temp. (°C)	K_{SV} ($10^5, \text{M}^{-1}$)	K_q ($10^{13}, \text{M}^{-1} \text{s}^{-1}$)	K_b ($10^5, \text{M}^{-1}$)	n
20	2.314 ± 0.098 ($R^2=0.97$)	4.628	1.549 ± 0.019 ($R^2=0.99$)	1.175
26	1.882 ± 0.065 ($R^2=0.98$)	3.764	1.425 ± 0.021 ($R^2=0.99$)	1.181
32	1.716 ± 0.071 ($R^2=0.98$)	3.342	1.409 ± 0.024 ($R^2=0.99$)	1.081
39	1.628 ± 0.043 ($R^2=0.99$)	3.256	1.331 ± 0.019 ($R^2=0.99$)	1.091

(Fig. 2B), indicating the formation of ground state complex between BSA and baicalein. The presence of BSA causes a red shift of 35 nm in the spectrum of baicalein, which supports the ground state complexation between BSA and baicalein (Fig. 2B). Thus, the possibility of involvement of a dynamical quenching mechanism can be neglected [34].

3.3. Binding constants and binding sites

The following Eq. (4) can be used to compute the binding constant (K_b) for static quenching interaction between protein and ligand, if there exists some equivalent independent binding sites in the protein [35,36]. It reveals the involvement of non-covalent forces in the binding of baicalein with BSA.

$$\log \frac{\Delta F}{F} = n \log [Q] + \log K_b \quad (4)$$

The values of K_b were estimated by plotting (Fig. 4A) $\log \frac{\Delta F}{F}$ versus $\log [Q]$ and are provided in Table 1. The values of K_b were found to be in the order of 10^5 M^{-1} and the number of binding sites (n) was calculated to be approximately one. The K_b of the interaction of baicalein with BSA was also estimated as $(1.23 \pm 0.03) \times 10^5$ ($R^2=0.99$) and $(3.02 \pm 0.02) \times 10^5$ ($R^2=0.99$) M^{-1} at pH 5 and 9, respectively, and the corresponding plot is given in Fig. S1. The binding constants at different pH conditions show that K_b values increase with the increase of pH. The higher the pH values, the higher the binding affinities of baicalein to BSA are. The associated changes in protein structure from pH 7.0 to pH 4.3 are known as N-F transition (N: native state and F: fast

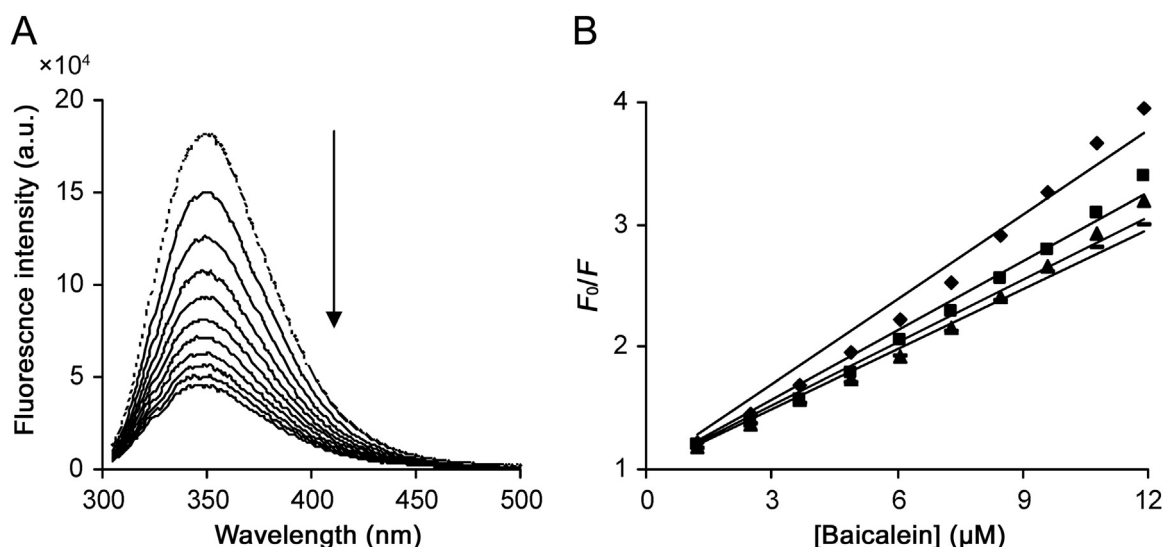


Fig. 3. (A) Fluorescence quenching spectra of BSA in the absence and presence of baicalein (0–12 μM) in 20 mM phosphate buffer of pH 7.0 at 26 °C and (B) the Stern-Volmer plot for the interaction of baicalein with BSA at different temperatures: (◆) 293 K, (■) 299 K (▲) 305 K (◻) 311 K. $\lambda_{\text{ex}}=295 \text{ nm}$.

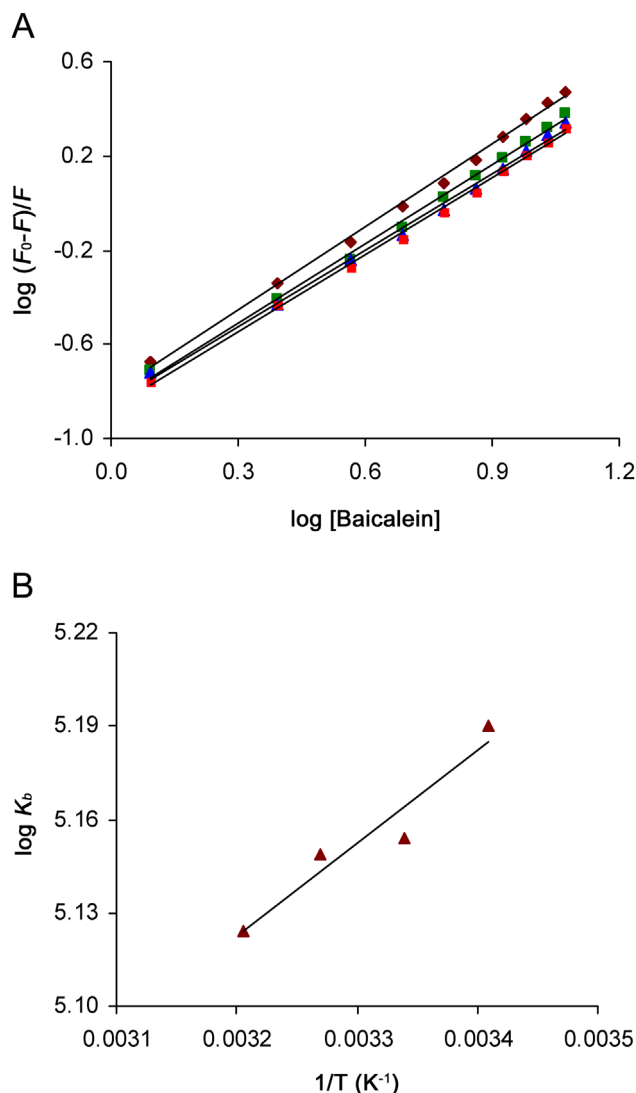


Fig. 4. (A) The double-logarithm plot for the interaction of baicalein with BSA at different temperatures: (◆) 293 K, (■) 299 K (▲) 305 K (●) 311 K. (B) The van't Hoff plot for the corresponding binding process.

Table 2

The binding constants for the interaction of baicalein with BSA in the presence of different KCl concentrations at 26 °C.

[KCl] (mM)	K_b (10^5 , M^{-1} , $R^2=0.99$)
0	1.425 ± 0.021
50	1.068 ± 0.011
100	0.912 ± 0.013
150	0.891 ± 0.016
200	0.818 ± 0.016

migrating state) and F state is actually obtained under pH 4.0 [37]. In the F state the secondary structure of BSA became partially disordered, but in pH 5, no such significant structural variation was reported for BSA [38]. The changes in pH from 7 to 9 caused N-B transition (B: basic state) in BSA, resulting in a perturbation of tertiary structure [38]. As per the pK_a value (5.3) [39], baicalein exists as a mixture of neutral and anionic forms at pH 7.0 [40]. It may be a notable reason for different binding affinities of baicalein towards BSA at pH 5. Similar results were reported in case of binding of baicalein with lysozyme by Li et al. [41]. Again the

protein structure was modified at pH 9.0 and it could be another prominent factor of different binding affinities of baicalein with BSA. The results showed that the anionic form had greater affinity towards BSA. From the point of bond dissociation energy (BDE) and proton dissociation energy (PDE) calculations, it is already established that 7 O–H is the easiest removable proton compared to 5 O–H and 6 O–H [42]. Hence at pH 7, the anion of baicalein (7 O–H) binds to the protein. The most stable anion [42] form of baicalein was docked with BSA and the results were discussed later in the molecular docking studies section. The binding constants in the presence of increasing KCl concentrations (Table 2) are obtained from the double-logarithm plot (Fig. S2A) and were found to be lower than K_b values without KCl (Fig. S2B). Fig. S2B shows the decrease in $\log K_b$ values with the increase in KCl concentrations, which reveals the presence of electrostatic interactions between baicalein and BSA.

The effects of SDS, CTAB and TX-100 on the binding of baicalein with BSA were also studied using fluorescence spectroscopy. The double-logarithm plots for the interaction of baicalein with BSA in the presence of the surfactants are given in Fig. S3. The reduction in values of K_b in case of SDS and CTAB was observed, but in case of TX-100 small increase occurred (Table S1). The decrease in K_b with the rise in temperature in all the cases indicates the involvement of static quenching in the absence and presence of the surfactants.

3.4. Effect of the metal ions on binding

The binding of baicalein with BSA was also analyzed in the presence of different common metal ions and it was noticed that the values of binding constant at 26 °C increased (Table 3). The K_b values were calculated according to Eq. (4) and the plots are presented in Fig. S4A. The UV–vis spectra of baicalein in the absence and presence of different metal ions are shown in Fig. S4B and the changes observed in the baicalein spectrum after addition of the metal ions indicate metal uptake by the baicalein. The increase of K_b value in the presence of metal ions can be attributed to the binding of metal–baicalein complexes to BSA [43,44]. However, the increase of K_b values for Ca^{2+} and Cu^{2+} is negligible in comparison to that for the other metal ions. Li et al. [20] reported that presence of Cu^{2+} ion decreased the binding efficacy of baicalein towards BSA. The changes in UV–vis spectra of BSA in the presence of these metal ions (Ca^{2+} , Mg^{2+} , Ni^{2+} , Mn^{2+} , Co^{2+} , Zn^{2+} and Cu^{2+}) have been reported earlier by us [45] and the binding affinities of these metal ions towards BSA were also estimated in the same report [45]. It was observed that the binding constants of the metal ions were less in comparison to the binding affinity of baicalein with BSA [44]. Another possible reason may be metal ion induced conformational changes of BSA (changes in UV–vis spectra of BSA in the presence of the metal ions) that facilitate binding of baicalein [43,44].

Table 3

The binding constants for the interaction of baicalein with BSA in the presence of different common metal ions at 26 °C.

Metal ions	K_b (10^5 , M^{-1} , $R^2=0.99$)
Without	1.42 ± 0.02
Ca^{2+}	1.49 ± 0.01
Mg^{2+}	1.71 ± 0.01
Mn^{2+}	1.55 ± 0.02
Fe^{2+}	1.92 ± 0.02
Co^{2+}	1.66 ± 0.02
Cu^{2+}	1.51 ± 0.03
Ni^{2+}	1.75 ± 0.01
Zn^{2+}	1.81 ± 0.01
Ag^+	1.56 ± 0.01

Table 4

Thermodynamic parameters for the interactions of baicalein with BSA in the absence and presence of surfactants.

Surfactant	Temperature (°C)	ΔG° (kJ/mol)	ΔH° (kJ/mol)	ΔS° (J/mol K)
No surfactant	20	-29.09	-5.66 ± 0.14	$+79.96 \pm 0.65$
	26	-29.57		
	32	-30.05		
	39	-30.61		
SDS	20	-27.35	-37.70 ± 0.24	-40.65 ± 0.87
	26	-27.11		
	32	-26.87		
	39	-26.58		
CTAB	20	-26.81	-10.04 ± 0.21	$+57.23 \pm 0.61$
	26	-27.18		
	32	-27.56		
	39	-27.99		
TX-100	20	-29.87	-7.79 ± 0.26	$+75.28 \pm 0.55$
	26	-30.31		
	32	-30.76		
	39	-31.28		

3.5. Binding modes

Assuming that the enthalpy change (ΔH°) does not vary appreciably over the temperature range, one can calculate ΔH° and ΔS° using the van't Hoff equation:

$$\log K_b = -\frac{\Delta H^\circ}{2.303RT} + \frac{\Delta S^\circ}{2.303R} \quad (5)$$

The free energy change (ΔG°) of interaction is calculated from ΔH° and ΔS° values using the following expression:

$$\Delta G^\circ = \Delta H^\circ - T\Delta S^\circ \quad (6)$$

The measured thermodynamic parameters associated with the interaction were estimated from the temperature dependence of the binding constant (K_b) using the Eqs. 5 and 6 and are listed in Table 4. The ΔH° and ΔS° values were determined from the slope and intercept of the van't Hoff plots (Fig. 4B and Fig. S5B). According to the sign and magnitude of the above parameters, Ross and Subramanian [46] analyzed a variety of interactions that play an important role in the protein-ligand association processes. The negative ΔH° (-5.66 ± 0.14 kJ/mol) and positive ΔS° ($+79.96 \pm 0.65$ J/mol K) for the binding of baicalein with BSA are associated with an electrostatic interaction followed by a hydrophobic force that causes a positive ΔS° change. We also investigated the type of interaction taking place between baicalein and surfactant molecules using a UV-vis study. The UV-vis spectra of baicalein are blue (4 nm) and red (20 nm) shifted in the presence of SDS and CTAB (Fig. S5A). The surfactant concentrations used were above their respective CMC values. These control experiments suggest that baicalein is hydrophobically associated with SDS and an electrostatic as well as hydrophobic association occurs between baicalein and CTAB.

The hydrophobic association of baicalein with SDS leads to a decrease in ΔS° (-40.65 ± 0.87 J/mol K) of the interaction between baicalein and BSA. As a consequence, the contribution of ΔH° increases from -5.66 ± 0.14 kJ/mol to -37.70 ± 0.24 kJ/mol, suggesting that only electrostatic interactions play a key role in the binding of baicalein with BSA in the presence of SDS. In the presence of the surfactant CTAB, the ΔH° values of the interactions become more negative, varying from -5.66 ± 0.14 to -10.04 ± 0.21 kJ/mol and ΔS° changes to $+57.23 \pm 0.61$ J/mol K from $+79.96 \pm 0.65$ J/mol K. This means that an electrostatic interaction occurs at pH 7 between baicalein and positively charged CTAB. In solution the availability of baicalein to BSA decreased due to its interaction with SDS and CTAB, consequently the binding constant reduced. In the presence of the non-ionic

surfactant TX-100, ΔH° changes to -7.79 ± 0.26 kJ/mol and the corresponding ΔS° to $+75.28 \pm 0.55$ J/mol K. The binding constants in the presence of TX-100 remain in the order of 10^5 M^{-1} , indicating that TX-100, unlike the charged surfactants, does not have significant effect on BSA-baicalein complex. The domain structure of BSA consists of three peptide segments parallel to each other forming a very long hydrophobic chain. Nozaki et al. [47] explained that SDS has a stronger affinity to the proteins compared to other cationic surfactants and binds to BSA via electrostatic and hydrophobic interactions [48]. It was observed that low concentrations of SDS stabilized the BSA structure whereas at higher concentrations it behaved as a denaturant [49]. Subdomain I (where Trp 134 resides) is more resistant to denaturation, but at the higher surfactant concentration unfolding of BSA occurs leading to the exposure of subdomain IIA (site 1, Trp 213 site).

The interaction affinities of the surfactants are reported in the following order: SDS > CTAB > TX-100 [50]. Hence, it can be concluded that the above order may be due to the relative protein denaturation order of the surfactants. Baicalein binds to site 1 (subdomain IIA) which is revealed by the site marker displacement studies as discussed in the following section (Preferential binding sites). The exposure of subdomain IIA diminishes the hydrophobic interaction of baicalein with BSA resulting in a negative ΔS° (-40.65 ± 0.87 J/mol K). Hence the combined effect of SDS (a denaturant and as a ligand of BSA) causes a decrease in the binding affinity of baicalein to BSA at different temperatures. The nonionic surfactant TX-100 binds to BSA via polar and nonpolar interaction modes [51]. Hence in the presence of TX-100 the entropic contributions decreases to some extent and the enthalpic part increases proportionally. Thus the presence of surfactants affects the binding affinity and binding mode of baicalein with BSA.

3.6. Preferential binding sites

Many ligand molecules bind to BSA at subdomains IIA and IIIA, although many lower affinity binding sites also exist. Site 1 (subdomain IIA) and site 2 (subdomain IIIA) correspond to the warfarin and ibuprofen binding sites [52,53]. The emission spectra of BSA bound to warfarin and ibuprofen excited at 295 nm in the presence of successive addition of baicalein are presented in Fig. 5A and B. The binding affinity of baicalein with BSA was estimated in the presence of warfarin and ibuprofen under similar experimental conditions and the corresponding plot is provided in Fig. 5C. It was found that the K_b values in the presence of warfarin decreased to $(9.36 \pm 0.51) \times 10^4 \text{ M}^{-1}$ from $(14.25 \pm 0.02) \times 10^4 \text{ M}^{-1}$ at 26 °C. However, in the presence of ibuprofen no such decrease was observed in the K_b value, $(16.63 \pm 0.158) \times 10^4 \text{ M}^{-1}$. Hence we conclude that baicalein binds to the hydrophobic site 1 (subdomain IIA), near to Trp 213 of BSA where warfarin binds, which was also proven by docking studies (discussed later). Baicalein does not compete with the ibuprofen binding site in BSA. Recent studies from our laboratory reveal the same kind of observations indicating the preferential binding of the ligands to site 1 (subdomain IIA) of HSA and BSA [54,55].

3.7. Energy transfer parameters

Förster non-radiative energy transfer theory is functional in many bio-systems to find out the distance (d) between the donor and acceptor. The energy transfer parameters ($J(\lambda)$, E , R and d) are calculated based on the equations reported earlier by various research groups [9,11,20] using the values of κ^2 (spatial orientation factor of the dipole), n (refractive index of the medium) and Q_D (fluorescence quantum yield of the donor) as 2/3, 1.336 and 0.118, respectively [34]. The parameter R is the critical distance between donor and acceptor when the energy transfer efficiency (E) is 50%.

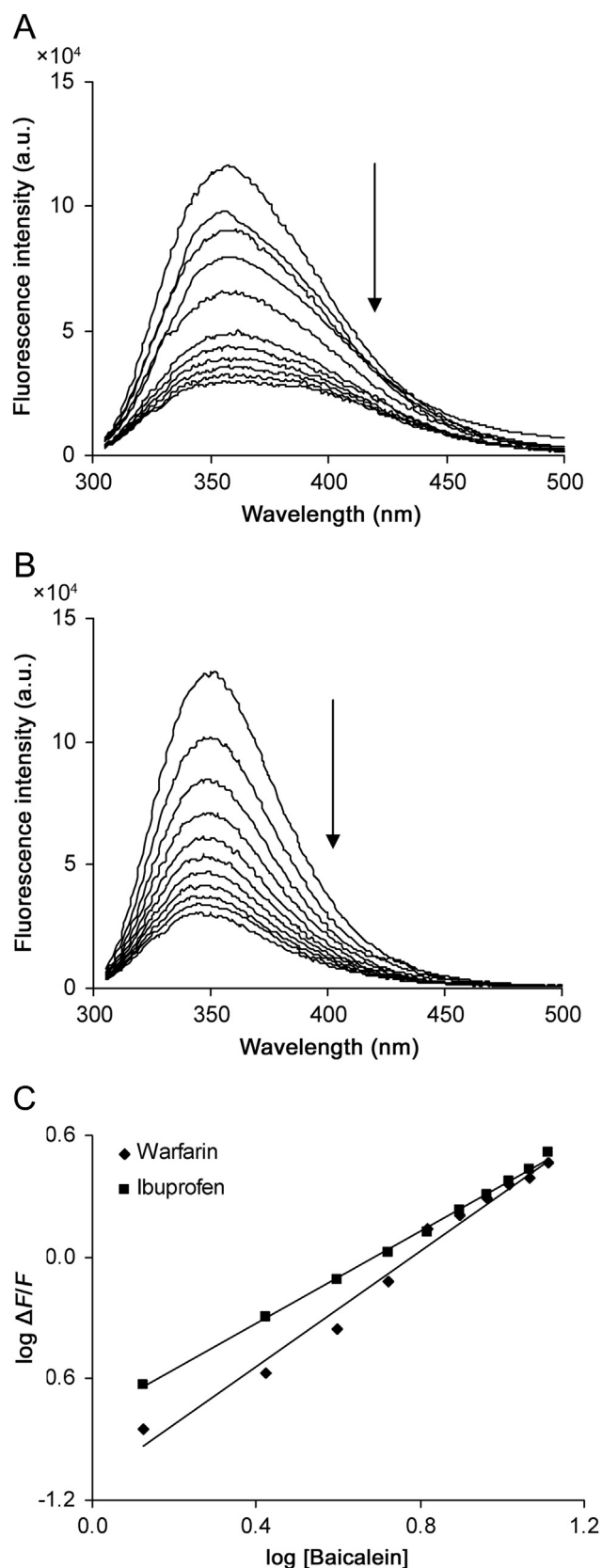


Fig. 5. The fluorescence emission spectra of BSA in the presence of (A) warfarin and (B) ibuprofen with successive addition of baicalein (0–12 μM) in 20 mM phosphate buffer of pH 7.0. $\lambda_{\text{ex}}=295 \text{ nm}$, $T=26 \text{ }^\circ\text{C}$. (C) Corresponding double-logarithm plots for the determination of binding constants in the presence of warfarin and ibuprofen.

The rate of energy transfer (K_{ET}) from BSA to baicalein at different temperatures was determined using the following equation [34].

$$K_{ET} = \tau_D^{-1} \left(\frac{R}{d} \right)^6 \quad (7)$$

where τ_D represents the lifetime of donor molecule.

The spectral overlap between the fluorescence emission of the protein and the UV-vis spectrum of baicalein in the absence and presence of the surfactants is presented in Fig. S6 and the energy transfer parameters are enlisted in Table S2. All the distances were calculated to be less than 7 nm and they were well settled in the range $0.5R_0 < d < 2R_0$, indicating the higher opportunity of energy transfer from Trp 213 to the ligands [34]. The rates of energy transfer in the absence and presence of the surfactants are provided in Table S2, which indicates that SDS and CTAB lower the rate with the increase of distance between donor and acceptor, but the non-ionic TX-100 increases the rate causing a lowering in the distance.

3.8. MALDI-TOF results

The complexation of baicalein with BSA was also established by the MALDI-TOF measurements. The pure BSA (from Sigma-Aldrich) showed the m/z at 66,479.54 Da and it was increased to 66,756.91 Da after complexation with baicalein (Fig. S7), indicating the possibility of a 1:1 binding between BSA and baicalein. It supports the value of n obtained from fluorescence data. Similar types of data were also reported in case of binding of triethoxy flavone and coumaroyltyramine with human serum albumin [56,57].

3.9. CD results

The characteristic α -helical configuration of BSA exhibits two negative bands at 208 and 222 nm in the far UV CD spectrum (Fig. S8). The binding between baicalein and BSA causes a slight increase in band intensity of the far UV CD without any notable shift of peaks at different wavelengths. It was found that the α -helical content of BSA changed from $(53.56 \pm 0.64)\%$ to $(54.81 \pm 0.31)\%$ and $(57.43 \pm 0.78)\%$ on 1:1 and 1:2 binding with baicalein respectively. The CD studies indicate that baicalein causes an increment in helix of the protein similar to the binding of genistein with BSA [45].

3.10. FT-IR results

Secondary structural components of proteins are monitored through the amide I band ($1700\text{--}1600 \text{ cm}^{-1}$). The other component in protein structures is the amide II band ($1575\text{--}1480 \text{ cm}^{-1}$) and provides less conformational sensitivity than amide I region [58,59]. The spectral shift in peaks of amide I and II bands of BSA at pH 7 (Fig. 6A) after binding with baicalein at molecular level indicates complexation between protein and ligand.

The secondary structural components of BSA before and after binding with baicalein were calculated and the results are summarized in Fig. S9. It was found that the percentage of α -helix of the protein increased from 51% to 53% and 55.7% upon 1:1 and 1:2 binding. The beta sheet content of the protein decreases from 31% to 27.2% upon binding with baicalein.

3.11. Explanation of hydrophobicity from FT-IR

The symmetric and asymmetric stretching vibrational frequencies of the non-polar groups, CH_2 and CH_3 (of BSA) in the region $3000\text{--}2800 \text{ cm}^{-1}$ [58,59], were shifted during interaction

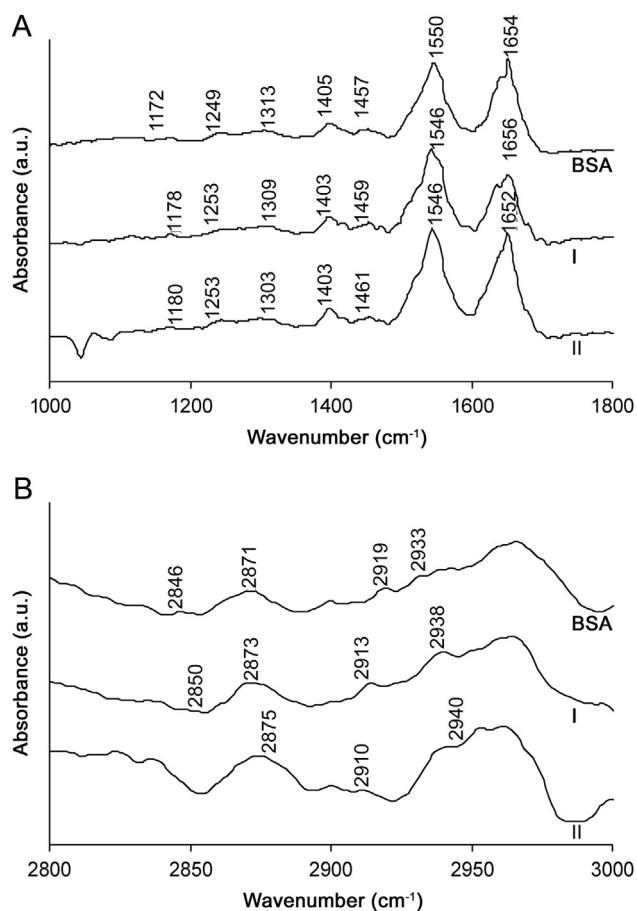


Fig. 6. FT-IR spectra of BSA and BSA bound with baicalein in the region (A) 1800–1000 cm^{-1} and (B) 3000–2800 cm^{-1} in 20 mM phosphate buffer of pH 7.0. The involvement of hydrophobic forces in the binding of baicalein with BSA was studied in the region of 3000–2800 cm^{-1} . (I) and (II) protein: ligand 1:1 and 1:2, respectively.

with baicalein (e.g. CH_2 asymmetric stretching frequency shifted from 2933 cm^{-1} of BSA to 2938 and 2940 cm^{-1} in 1:1 and 1:2 complexes with baicalein, Fig. 6B). The result indicates the presence of a hydrophobic association between BSA and baicalein [59,60].

3.12. Three-dimensional fluorescence

The 3D fluorescence technique can provide some information regarding the changes in conformation of the proteins during ligand binding. The 3D spectrum of BSA (Fig. S10A) exhibits distinct peak 1 and peak 2 which got quenched after interaction with baicalein. The peak 1 is the originality of tryptophan and tyrosine residues and peak 2 presents the spectral properties of polypeptide backbone of the protein [45,61]. The results are provided in Table S3, which clearly indicate that a blue shift (20 nm) in the presence of baicalein induced some micro-environmental (hydrophobic interactions between aromatic ring and the hydrophobic residues) and conformational changes in the BSA structure [45,61].

3.13. Unfolding and refolding study

The denaturation of BSA using urea was carried out in the absence and presence of baicalein to investigate the structural stability of BSA. BSA was excited at 295 nm and the emissions were recorded at 347 nm for the data analyses. The curve of F/F_0 against

urea concentrations in the absence of baicalein lies under the curve when baicalein is present in the medium (Fig. 7C), indicating the stabilization of BSA even in the presence of chemical denaturant [62]. The chemical denaturation of BSA using urea and urea-baicalein system caused a gradual decrease in the intrinsic fluorescence intensity (Fig. 7) of BSA with a red shift of 7 nm in each of the cases, which resembles the fluorescence emission spectra of L-tryptophan in aqueous buffer system [63]. The denaturation of BSA caused the exposure of the buried tryptophan (Trp 213) to a more polar environment. The refolding experiments of BSA were performed by diluting the actual denatured BSA solution and the fluorescence intensities along with the peak positions were compared with the native BSA (Fig. 8). The native BSA did not show any changes in emission maxima except a reduction in the fluorescence intensity due to dilution. The diluted denatured BSA in the absence and presence of baicalein exhibits significant blue shift to 347 nm (Fig. 8), indicating the refolding after dilution [64,65].

The steady-state fluorescence measurements of unfolding and refolding of BSA were also confirmed using fluorescence lifetime estimation. The lifetime decay for BSA (Fig. S11) was fitted as a bi-exponential decay function to calculate the lifetime data [66]. The average fluorescence lifetime of BSA in native state was found to be (5.25 ± 0.21) ns, which was higher than the average lifetime of L-tryptophan (3.86 ns) in aqueous buffer solution [63]. The decrease in the average lifetime of BSA (4.65 ± 0.14 ns) in the presence of baicalein (15 μM) is indicative of the excited state complex formation besides a ground state association. The quenching constants are greater than the limiting value ($2 \times 10^{10} \text{ M}^{-1} \text{ s}^{-1}$) of dynamical quenching parameters in aqueous solution, which rules out the involvement of dynamic quenching. The presence of 7 M urea leads to a decrease in the average lifetime of BSA both in the absence (2.81 ± 0.11 ns) and presence (2.78 ± 0.05 ns) of baicalein. The refolding experiment of BSA from its denatured state was performed using dilution method and the lifetime data were considered for further discussion. After dilution the average lifetime of denatured BSA in the absence and presence of baicalein goes on increasing to 3.23 ± 0.17 ns, and 3.09 ± 0.09 ns, respectively, which clearly signifies the refolding of BSA towards a partially folded state [63,66]. All the lifetime data are provided in Table S4.

3.14. Molecular docking results

Molecular docking was executed to substantiate the experimental results. The stereoview of the docked pose of the ligand with BSA is given in Fig. 9A. The inner hub of BSA (site 1, subdomain IIA) is hydrophobic and the entrance of the hub is enclosed by the polar amino acid residues such as Arg 194, Arg 198, Arg 217 and Lys 221. The ring C of baicalein is very close to Trp 213 and the distances of its 1-O atom to Trp 213 is 6.6 Å. It can be concluded that baicalein binds to the hydrophobic pocket near to Trp 213 (site 1, subdomain IIA) and involvement of Arg 194, Arg 217 and Asp 450 contributes to the electrostatic forces in the protein-ligand complex. The distances of some residues of BSA from baicalein are given in Table 5. We calculated ASA for free BSA and the baicalein-BSA complex and the results are listed in Table 5. The binding of baicalein within the central hub of different helical regions of assorted subdomains near to Trp 213 of BSA may be attributed to the helical stabilization properties of baicalein [67,68].

The most stable anionic form of the baicalein is docked with BSA (Fig. 9B). The anion is binding at the same site where molecular baicalein binds. The distances from baicalein and its anion from the amino acids residues are provided in Fig. 9C and D. The experimental results show that baicalein anion has a greater binding affinity towards BSA. The program for energetic analysis of

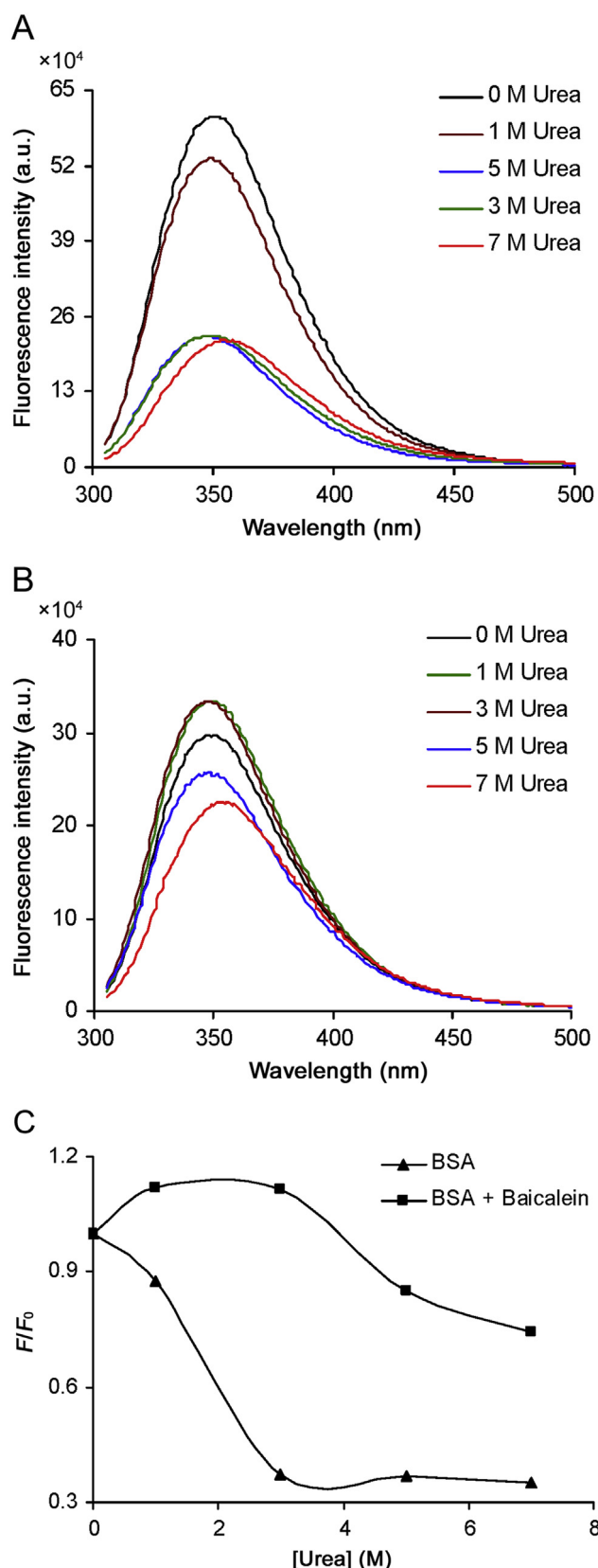


Fig. 7. Fluorescence emission spectra of (A) BSA (15 μM) and (B) BSA-baicalein (15 μM:15 μM) system against various urea concentrations. $\lambda_{\text{ex}}=295$ nm; (C) The corresponding variations in F/F_0 against the increasing concentration of urea.

receptor-ligand system (PEARLS) [69] was used to determine the theoretical values of free energy of binding for baicalein and its anionic form with native BSA. The total score (protein-ligand

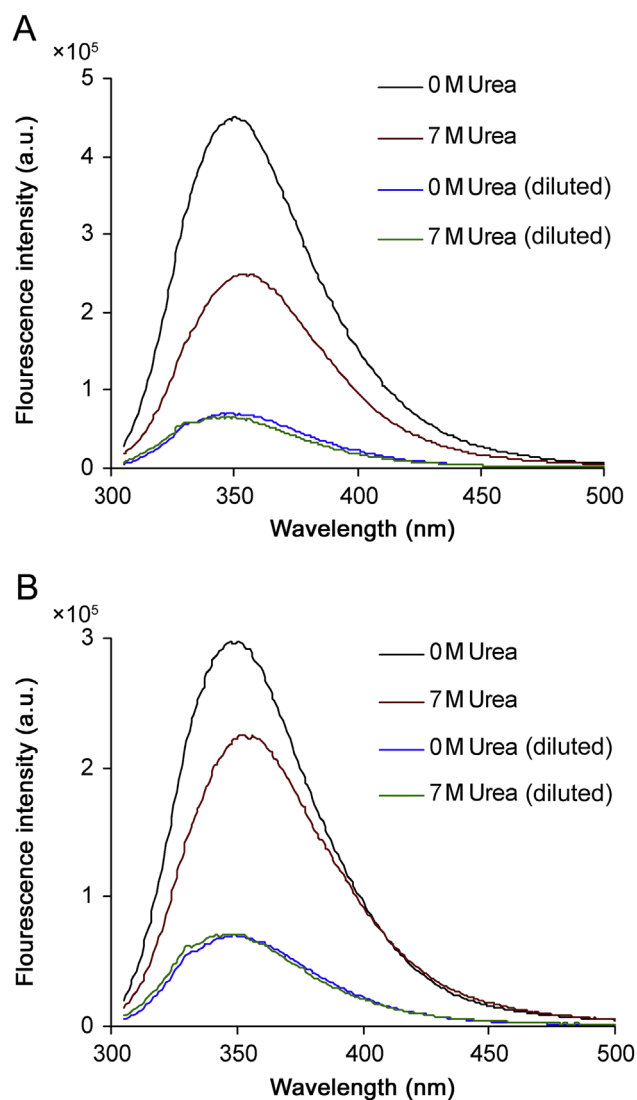


Fig. 8. Emission spectra of (A) BSA and (B) BSA-baicalein system during refolding before and after dilution in the presence of urea. $\lambda_{\text{ex}}=295$ nm.

binding free energy) obtained from the docking studies of baicalein and its anion with BSA is -10.79 and -14.63 , respectively, which shows that the anionic form has a higher affinity towards BSA. PEARLS data (protein-ligand binding free energy) indicates the similar kind of results where the total protein-ligand binding energy was calculated to be -7.04 and -10.79 kcal/mol for baicalein and its anion, respectively, which is also in favour of the previous results.

4. Conclusion

In this report the binding of baicalein with BSA was studied using UV-vis, fluorescence, CD, FT-IR and molecular docking methods. The interaction of baicalein with BSA occurs through electrostatic interactions along with hydrophobic forces that results in a positive entropy ($+79.96 \pm 0.65$ J/mol K) change during complexation. The molecular docking studies in accordance with the experimental results are sufficient to prove the mode of binding taking place between BSA and baicalein. The binding affinity of baicalein towards BSA is reduced about 43% in the presence of 200 mM KCl, indicating the involvement of electrostatic interaction in the protein-ligand complex. The effects of SDS, CTAB

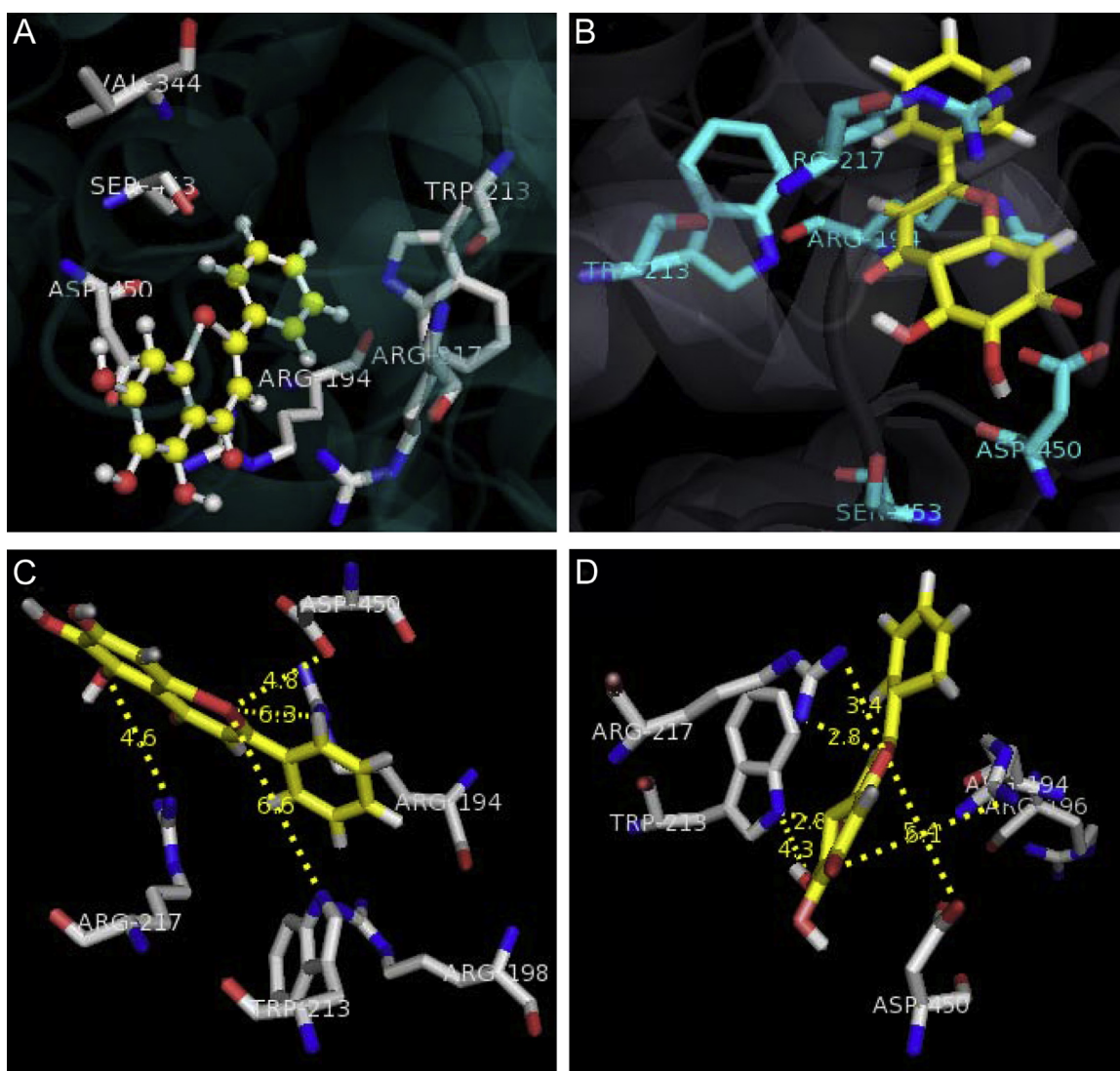


Fig. 9. The docked conformation of (A) baicalein and (B) baicalein anion with BSA, and the bonding distances of (C) baicalein and (D) its anion from the polar amino acid residues of the protein.

Table 5

Distances (Å) of some amino acid residues of BSA from baicalein in the docked pose and the change in accessible surface area (Δ ASA) of the interacting residues of BSA (uncomplexed) and their complex with baicalein.

Residues	Distance (Å)	Δ ASA (Å ²)
Arg 194 N η 1	5.0 [4-C=O]	25.11
N η 2	5.3 [4-C=O]	
Leu 197		14.93
Trp 213 (N ϵ)	6.6 [1-O]	23.65
	7.8 [4-C=O]	
Arg 217 N η 1	2.7 [4-C=O]	29.14
N η 2	3.8 [4-C=O]	
N η 1	4.6 [5-O]	
N η 2	5.4 [5-O]	
Val 342	–	26.01
Asp 450 O δ 1	4.8 [1-O]	30.47
O δ 2	5.3 [1-O]	
Ser 453	–	5.32

and TX-100 were also monitored. In the presence of SDS and CTAB the binding constants of baicalein with BSA at different temperatures decreased and SDS suppressed the hydrophobic forces and the interaction became completely electrostatic in nature. CTAB as a cationic surfactant also enhanced the electrostatic forces and

reduced the contribution of hydrophobic forces. The non-ionic surfactant TX-100 did not alter the mode of binding between baicalein and BSA. The presence of metal ions enhanced the binding affinity of baicalein towards BSA. This indicates a longer lifetime of baicalein in blood in the presence of metal ions and the corresponding effectiveness will increase. From the Förster's theory, it has been established that the distance of baicalein from Trp 213 is 3.27 nm, which predicts that there is a probability of energy transfer from the donor Trp moiety to the acceptor baicalein molecule. The negative ΔG° reveals the spontaneous nature of complexation processes between baicalein and BSA in the absence or presence of surfactants at different temperatures. These studies are significant as they provide useful information of the binding of serum proteins with biologically active components.

Acknowledgments

Swagata Dasgupta is grateful to Department of Science and Technology (DST, Project no. SR/SO/BB-54/2007), Government of India for financial support. The authors want to thank the Central Research Facility, IIT Kharagpur for providing CD and FT-IR facilities. Atanu Singha Roy and Amit Kumar Dinda thank CSIR, New

Delhi and Nitin Kumar Pandey thanks IIT Kharagpur for Senior Research Fellowships.

Appendix A. Supporting information

Supplementary data associated with this article can be found in the online version at <http://dx.doi.org/10.1016/j.jpha.2016.04.001>.

References

- [1] U. Kragh-Hansen, Molecular aspects of ligand binding serum albumin, *Pharmacol. Rev.* 33 (1981) 17–53.
- [2] P.A. Zunszain, J. Ghuman, T. Komatsu, et al., Crystal structural analysis of human serum albumin complexed with hemin and fatty acids, *BMC Struct. Biol.* 3 (2003) 6–14.
- [3] S. Sugio, A. Kashima, S. Mochizuki, et al., Crystal structure of human serum albumin at 2.5 Å resolution, *Protein Eng.* 12 (1999) 439–446.
- [4] D.C. Carter, B. Chang, J.X. Ho, et al., Preliminary crystallographic studies of four crystal forms of serum albumin, *Eur. J. Biochem.* 226 (1994) 1049–1052.
- [5] H.M. He, D.C. Carter, Atomic structure and chemistry of human serum albumin, *Nature* 358 (1992) 209–215.
- [6] I. Petitpas, A.A. Bhattacharya, S. Twine, et al., Crystal structure analysis of warfarin binding to human serum albumin: anatomy of drug site I, *J. Biol. Chem.* 276 (2001) 22804–22809.
- [7] J. Ghuman, P.A. Zunszain, I. Petitpas, et al., Crystal structure analysis of warfarin binding to human serum albumin. Anatomy of drug site I, *J. Mol. Biol.* 353 (2005) 38–52.
- [8] B.F. Peterman, K.J. Laidler, Study of reactivity of tryptophan residues in serum albumins and lysozyme by N-bromosuccinamide fluorescence quenching, *Arch. Biochem. Biophys.* 199 (1980) 158–164.
- [9] I. Matei, S. Ionescu, M. Hillebrand, Interaction of fisetin with human serum albumin by fluorescence, circular dichroism spectroscopy and DFT calculations: binding parameters and conformational changes, *J. Lumin.* 131 (2011) 1629–1635.
- [10] A. Singha Roy, D.R. Tripathy, A. Chatterjee, et al., A spectroscopic study of the interaction of the antioxidant naringin with bovine serum albumin, *J. Biophys. Chem.* 1 (2010) 141–152.
- [11] I. Matei, M. Hillebrand, Interaction of kaempferol with human serum albumin: a fluorescence and circular dichroism study, *J. Pharm. Biomed. Anal.* 51 (2010) 768–773.
- [12] L. Wang, Y. Ling, Y. Chen, et al., Flavonoid baicalein suppresses adhesion, migration and invasion of MDA-MB-231 human breast cancer cells, *Cancer Lett.* 297 (2010) 42–48.
- [13] J.D. Deschamps, V.A. Kenyon, T.R. Holman, Baicalein is a potent in vitro inhibitor against both reticulocyte 15-human and platelet 12-human lipoxigenases, *Bioorg. Med. Chem.* 14 (2006) 4295–4301.
- [14] P. Pu, X.A. Wang, M. Salim, et al., Baicalein, a natural product, selectively activating AMPK α (2) and ameliorates metabolic disorder in diet-induced mice, *Mol. Cell. Endocrinol.* 262 (2012) 128–138.
- [15] R.R. Liang, S. Zhang, J.A. Qi, et al., Preferential inhibition of hepatocellular carcinoma by the flavonoid Baicalein through blocking MEK-ERK signaling, *Int. J. Oncol.* 41 (2012) 969–978.
- [16] Z. Zhang, W. Cui, G. Li, et al., Baicalein protects against 6-OHDA-induced neurotoxicity through activation of Keap1/Nrf2/HO-1 and involving PKC α and PI3K/AKT signaling pathways, *J. Agric. Food Chem.* 60 (2012) 8171–8182.
- [17] K.S. Oh, B.K. Oh, C.H. Park, et al., Baicalein potently inhibits Rho kinase activity and suppresses actin stress fiber formation in angiotensin II-stimulated H9c2 cells, *Biol. Pharm. Bull.* 35 (2012) 1281–1286.
- [18] J. Xiao, G. Kai, A review of dietary polyphenol-plasma protein interactions: characterization, influence on the bioactivity, and structure-affinity relationship, *Crit. Rev. Food Sci. Nutr.* 52 (2012) 85–101.
- [19] J. Xiao, Polyphenol-plasma proteins interaction: its nature, analytical techniques, and influence on bioactivities of polyphenols, *Curr. Drug Metab.* 14 (2013) 367–368.
- [20] D. Li, M. Zhu, C. Xu, et al., Characterization of the baicalein-bovine serum albumin complex without or with Cu²⁺ or Fe³⁺ by spectroscopic approaches, *Eur. J. Med. Chem.* 46 (2011) 588–599.
- [21] C.N. Pace, F. Vajdos, L. Fee, et al., How to measure and predict the molar absorption coefficient of a protein? *Protein Sci.* 4 (1995) 2411–2423.
- [22] J.L. Perry, M.R. Goldsmith, T.R. Williams, et al., Binding of warfarin influences the acid-base equilibrium of H242 in sudlow site I of human serum albumin, *Photochem. Photobiol.* 82 (2006) 1365–1369.
- [23] J.H. Tang, F. Luan, X.G. Chen, Binding analysis of glycyrrhetic acid to human serum albumin: fluorescence spectroscopy, FT-IR, and molecular modeling, *Bioorg. Med. Chem.* 14 (2006) 3210–3217.
- [24] L. Whitmore, B.A. Wallace, DICHROWEB: an online server for protein secondary structure analyses from circular dichroism spectroscopic data, *Nucleic Acids Res.* 32 (2004) W668–W673.
- [25] D.M. Byler, H. Susi, Examination of the secondary structure of proteins by deconvoluted FT-IR spectra, *Biopolymers* 25 (1986) 469–487.
- [26] A. Bujacz, Structures of bovine, equine and leporine serum albumin, *Acta Crystallogr. D* 68 (2012) 1278–1289.
- [27] H.M. Berman, J. Westbrook, Z. Feng, et al., The protein data bank, *Nucleic Acids Res.* 28 (2000) 235–242.
- [28] W.L. DeLano, The PyMol molecular graphics system, DeLano Scientific, San Carlos, CA, USA, 2004, (<http://www.pymol.sourceforge.net>).
- [29] S.J. Hubbard, J.M. Thornton, NACCESS. Computer program, Department of Biochemistry and Molecular Biology, University College of London, 1993.
- [30] B.K. Sahoo, K.S. Ghosh, S. Dasgupta, Investigating the binding of curcumin derivatives to bovine serum albumin, *Biophys. Chem.* 132 (2008) 81–88.
- [31] T.J. Mabry, K.R. Markham, M.B. Thomas, *The Systematic Identification of Flavonoids*, Springer-Verlag, New York 1970, pp. 41–164.
- [32] F. Zsila, Z. Bikadi, M. Simonyi, Probing the binding of the flavonoid, quercetin to human serum albumin by circular dichroism, electronic absorption spectroscopy and molecular modeling studies, *Biochem. Pharmacol.* 65 (2003) 447–456.
- [33] H.A. Benesi, J.H. Hildebrand, A spectrophotometric investigation of the interaction of iodine with aromatic hydrocarbons, *J. Am. Chem. Soc.* 71 (1949) 2703–2707.
- [34] J.R. Lakowicz, *Principles of Fluorescence Spectroscopy*, Springer, New York 2006, pp. 278–284.
- [35] S. Bi, L. Yan, Y. Sun, et al., Investigation of ketoprofen binding to human serum albumin by spectral methods, *Spectrochim. Acta A* 78 (2011) 410–414.
- [36] Z. Chi, R. Liu, Phenotypic characterization of the binding of tetracycline to human serum albumin, *Biomacromolecules* 12 (2011) 203–209.
- [37] T.J. Su, J.R. Lu, R.K. Thomas, et al., The conformational structure of bovine serum albumin layers adsorbed at the silica-water interface, *J. Phys. Chem. B* 102 (1998) 8100–8108.
- [38] A. Michnik, K. Michalik, Z. Drzazga, Stability of bovine serum albumin at different pH, *J. Therm. Anal. Calorim.* 80 (2005) 399–406.
- [39] K. Yoshizuka, H. Ohta, K. Inoue, et al., Selective separation of flavonoids with a polyvinyl alcohol membrane, *J. Membr. Sci.* 118 (1996) 41–48.
- [40] M.X. Xie, X.Y. Xu, Y.D. Wang, Interaction between hesperetin and human serum albumin revealed by spectroscopic methods, *Biochim. Biophys. Acta* 1724 (2005) 215–224.
- [41] D. Li, T. Zhang, B.C. Xu, et al., Effect of pH on the interaction of baicalein with lysozyme by spectroscopic approaches, *J. Photochem. Photobiol. B: Biol.* 104 (2011) 414–424.
- [42] Z.S. Marković, J.M.D. Marković, D. Milenković, et al., Mechanistic study of the structure-activity relationship for the free radical scavenging activity of baicalein, *J. Mol. Model.* 17 (2011) 2575–2584.
- [43] J.B. Xiao, J. Shi, H. Cao, et al., Analysis of binding interaction between puerarin and bovine serum albumin by multi-spectroscopic method, *J. Pharm. Biomed. Anal.* 45 (2007) 609–615.
- [44] D. Li, Y. Wang, J. Chen, et al., Characterization of the interaction between farrerol and bovine serum albumin by fluorescence and circular dichroism, *Spectrochim. Acta A* 79 (2011) 680–686.
- [45] A. Singha Roy, D.R. Tripathy, A. Chatterjee, et al., The influence of common metal ions on the interactions of the isoflavone genistein with bovine serum albumin, *Spectrochim. Acta A* 102 (2013) 393–402.
- [46] P.D. Ross, S. Subramanian, Thermodynamics of protein association reactions: forces contributing to stability, *Biochemistry* 20 (1981) 3096–3102.
- [47] Y. Nozaki, J.A. Reynolds, C. Tanford, Interaction of a cationic detergent with bovine serum-albumin and other proteins, *J. Biol. Chem.* 249 (1974) 4452–4459.
- [48] A.D. Nielsen, K. Borch, P. Westh, Thermochemistry of the specific binding of C12 surfactants to bovine serum albumin, *Biochim. Biophys. Acta* 1479 (2000) 321–331.
- [49] S. Deep, J.C. Ahluwalia, Interaction of bovine serum albumin with anionic surfactants, *Phys. Chem. Chem. Phys.* 3 (2001) 4583–4591.
- [50] Z.G. Yaseen, On the interactions of bovine serum albumin with some surfactants: New insights from conductivity studies, *J. Chem. Pharm. Res.* 4 (2012) 3361–3367.
- [51] S.K. Singh, N. Kishore, Thermodynamic insights into the binding of triton X-100 to globular proteins: a calorimetric and spectroscopic investigation, *J. Phys. Chem. B* 110 (2006) 9728–9737.
- [52] G. Sudlow, D.J. Birkett, D.N. Wade, The characterization of two specific drug binding sites on human serum albumin, *Mol. Pharmacol.* 11 (1975) 824–832.
- [53] G. Sudlow, D.J. Birkett, D.N. Wade, Further characterization of specific drug binding sites on human serum albumin, *Mol. Pharmacol.* 12 (1976) 1052–1061.
- [54] A. Singha Roy, K.S. Ghosh, S. Dasgupta, An investigation into the altered binding mode of green tea polyphenols with human serum albumin on complexation with copper, *J. Biomol. Struct. Dyn.* 31 (2013) 1191–1206.
- [55] A. Singha Roy, N.K. Pandey, S. Dasgupta, Preferential binding of fisetin to the native state of bovine serum albumin: spectroscopic and docking studies, *Mol. Biol. Rep.* 40 (2013) 3239–3253.
- [56] M. Gokara, B. Sudhamalla, D.G. Amroo, et al., Molecular interaction studies of trimethoxy flavone with human serum albumin, *Plos One* 5 (2010) e8834.
- [57] S. Neelam, M. Gokara, B. Sudhamalla, et al., Interaction studies of coumaroyltyramine with human serum albumin and its biological importance, *J. Phys. Chem. B* 114 (2010) 3005–3012.
- [58] A. Elliott, E.J. Ambrose, Structure of synthetic polypeptides, *Nature* 165 (1950) 921–922.
- [59] S. Krimm, J. Bandekar, Vibrational spectroscopy and conformation of peptides,

- polypeptides and proteins, *Adv. Protein Chem.* 38 (1986) 181–364.
- [60] P. Bourassa, C.D. Kanakis, P. Tarantilis, et al., Resveratrol, genistein, and curcumin bind bovine serum albumin, *J. Phys. Chem. B* 114 (2010) 3348–3354.
- [61] B. Sandhya, A.H. Hedge, S.S. Klankur, et al., Interaction of tripolidine hydrochloride with serum albumins: Thermodynamic and binding characteristics, and influence of site probes, *J. Pharm. Biomed. Anal.* 54 (2011) 1180–1186.
- [62] B.K. Paul, A. Samanta, N. Guchhait, Exploring hydrophobic subdomain IIA of the protein bovine serum albumin in the native, intermediate, unfolded, and refolded states by a small fluorescence molecular reporter, *J. Phys. Chem. B* 114 (2010) 6183–6196.
- [63] D. Patra, C. Barakat, R.M. Tafach, Study on effect of lipophilic curcumin on subdomain IIA site of human serum albumin during unfolded and refolded states: a synchronous fluorescence spectroscopic study, *Colloids Surf. B* 94 (2012) 351–361.
- [64] C. Barakat, D. Patra, Combining time-resolved fluorescence with synchronous fluorescence spectroscopy to study bovine serum albumin–curcumin complex during unfolding and refolding processes, *Luminescence* 28 (2012) 149–155.
- [65] B. Ojha, G. Das, The interaction of 5-(alkoxy)naphthalen-1-amine with bovine serum albumin its effect on the conformation of protein, *J. Phys. Chem. B* 114 (2010) 3979–3986.
- [66] O.K. Abou-Zied, O.I.K. Al-Shihi, Characterization of subdomain IIA binding site of human serum albumin in its native, unfolded and refolded states using small molecular probes, *J. Am. Chem. Soc.* 130 (2008) 10793–10801.
- [67] D. Roy, S. Dutta, S.S. Maity, et al., Spectroscopic and docking studies of the binding of two stereoisomeric antioxidant catechins to serum albumins, *J. Lumin.* 132 (2012) 1364–1375.
- [68] A. Singha Roy, D.R. Tripathy, S. Dasgupta, An alternate mode of binding of the polyphenol quercetin with serum albumins when complexed with Cu(II), *J. Lumin.* 132 (2012) 2943–2951.
- [69] L.Y. Han, H.H. Lin, Z.R. Li, et al., PEARLS: program for energetic analysis of receptor–ligand system, *J. Chem. Inf. Model.* 46 (2006) 445–450.